

Clay B. Blankenship\*  
Naval Research Laboratory, Monterey, California

## 1. INTRODUCTION

A method to simultaneously retrieve cloud liquid water and water vapor profiles using data from the Advanced Microwave Sounding Unit-B (AMSU-B) radiometer is described. Results of simulated retrievals for simple liquid and mixed-phase clouds and global maps of retrieved cloud parameters are presented. The AMSU-B, with channels at  $183.31 \pm 1$ ,  $\pm 3$ ,  $\pm 7$ , 150, and 91 GHz, can be used to retrieve water vapor profiles, taking advantage of the 183.31 GHz water vapor absorption line. The retrieval, a physical inversion using an optimal estimation technique, is extended to retrieve limited cloud liquid water profiling information as well.

## 2. RETRIEVAL ALGORITHM

The basic retrieval algorithm, a physical iterative retrieval of water vapor profile, is described in Blankenship et al. (2000). This method has been adapted to execute a combined retrieval of liquid cloud and water vapor profiles. The algorithm attempts to find the best fit to the AMSU-B observed brightness temperatures as well as to a background profile—in this case given by an analysis from the Navy Operational Global Atmospheric Prediction System (NOGAPS). Currently the AMSU-B channels at  $183 \pm 1$ , 3, 7; and 150 GHz are used as inputs.

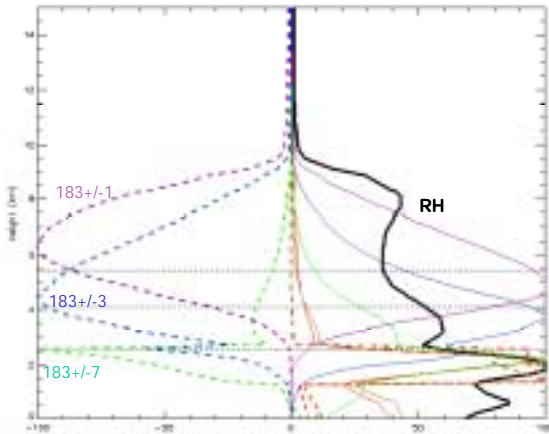


**Figure 1.** Normalized weighting functions (solid lines) for the profile given by the thick black line (RH), with a cloud at 2 km where RH=100%. Jacobians (dashed) show levels for which the observations are sensitive to changes in RH'.

\*Corresponding author address: Clay B. Blankenship, Naval Research Laboratory, Monterey, CA 93943; e-mail: blankens@nrlmry.navy.mil.

The algorithm tries to minimize the cost function

$$J(x) = (\mathbf{y} - \mathbf{H}(\mathbf{x}))^T \mathbf{S}_e^{-1} (\mathbf{y} - \mathbf{H}(\mathbf{x})) + (\mathbf{x} - \mathbf{x}_b)^T \mathbf{S}_a^{-1} (\mathbf{x} - \mathbf{x}_b)$$

where  $\mathbf{y}$  is the vector of observations (brightness temperatures),  $\mathbf{H}$  is the forward model,  $\mathbf{S}_e$  is the observed plus forward model error covariance matrix,  $\mathbf{x}$  is the atmospheric state vector,  $\mathbf{x}_b$  is the background state, and  $\mathbf{S}_a$  is the background error covariance matrix. This is equivalent to maximizing the Bayesian probability of atmospheric state  $\mathbf{x}$  given knowledge of  $\mathbf{x}_b$ ,  $\mathbf{y}$ , and their error characteristics (Rodgers, 2000). We solve for a new  $\mathbf{x}$  which minimizes this function using a linearization of  $\mathbf{H}(\mathbf{x})$  about the current  $\mathbf{x}$ . This process is repeated until convergence is obtained. If the retrieval fails to converge within 12 iterations it is rejected, but most converge in 3 to 6 iterations.

In the combined water vapor/cloud profile retrieval, the state vector  $\mathbf{x}$  is defined as a pseudohumidity variable RH', equal to relative humidity (RH) when RH<100% and linearly related to cloud liquid water density when clouds exist. (Saturation is assumed over the entire scene in this case.)

$$\begin{aligned} \text{RH}' &= \text{RH} \text{ (unsaturated)} \\ \text{RH}' &= 1.00 + k \cdot \text{CLW} \text{ (saturated)}. \end{aligned}$$

Here CLW refers to cloud liquid water. Since the Jacobian terms  $\partial \text{TB} / \partial \text{RH}$  and  $\partial \text{TB} / \partial \text{CLW}$  are known, the Jacobian term  $\partial \text{TB} / \partial \text{RH}'$  can be calculated from these relationships. A value of  $k = 6.667 \cdot 10^5$  was chosen (for CLW expressed in kg/kg) to give the right order of magnitude to the Jacobian term for cloudy layers. Discontinuities at RH=100% cannot be eliminated because one value of  $k$  must be used at all frequencies.

The Jacobians are plotted in Figure 1 for a profile with a cloud at 2 km. The  $183 \pm 3$  and  $\pm 7$  GHz channels have secondary peaks at the top of the cloud, indicating sensitivity to the cloud liquid water at that level. The 91 and 150 GHz channels have the highest sensitivity throughout the cloud, rather than at the ground as in the cloud-free case.

A plane parallel, non-precipitating liquid or mixed-phase cloud is assumed with an upper limit of 0.5 mm of cloud liquid water. Scattering is neglected; the presence of precipitation will generally cause the retrieval to fail due to high TB error.

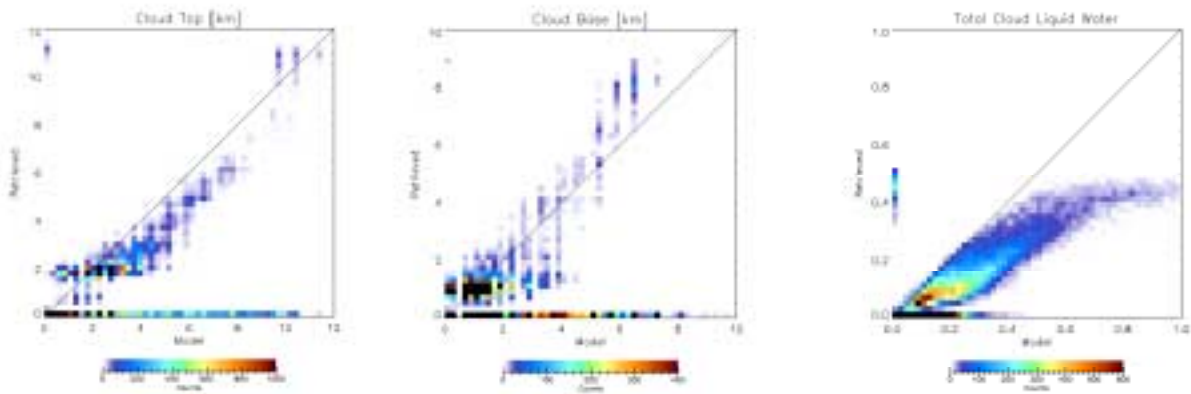
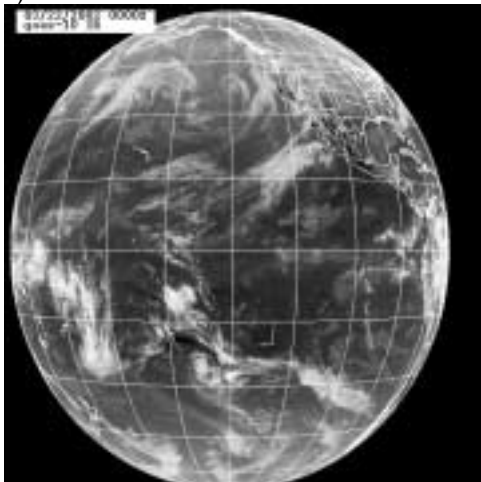
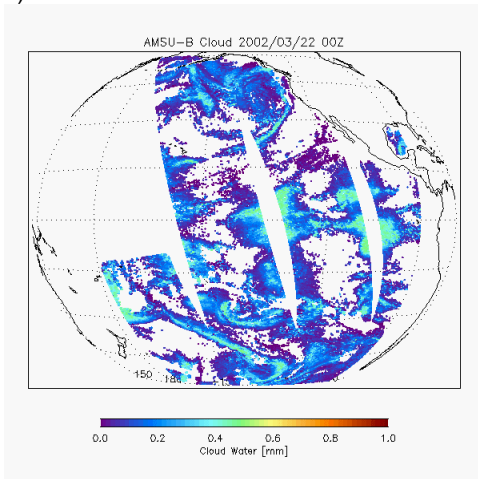


**Figure 2.** Retrieved versus true cloud parameters for simulated retrievals. a) Cloud top; b) Cloud base; c) Cloud Liquid Water.

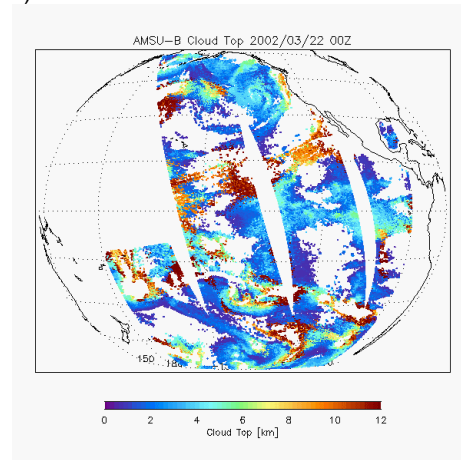
a)



b)



c)



d)

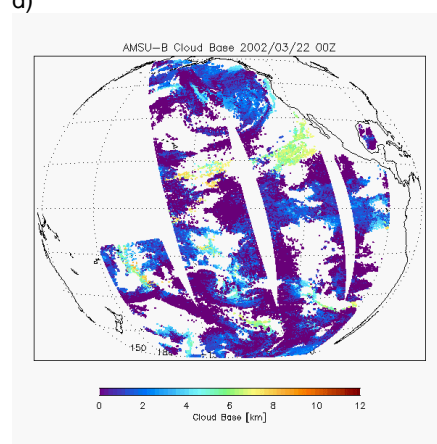


**Figure 3.** a) GOES-10 infrared image; b) Retrieved cloud liquid water; c) Retrieved cloud top; d) Retrieved cloud base.

### 3. SIMULATIONS

Retrievals were performed using observations simulated from a database of ECMWF analysis temperature, humidity, and cloud profiles. The cloud profiles were adjusted to be plane parallel by removing layers of low cloud fraction and assuming that the remaining layers had 100% cloud cover. Results from simulated retrievals are shown in Figure 2. Simulated retrievals are able to reproduce cloud top, base, and liquid water amount fairly well, with cloud top being slightly underestimated, cloud base slightly overestimated, and total cloud liquid water somewhat underestimated on average.

### 4. RETRIEVALS FROM AMSU-B OBSERVATIONS

Retrievals were performed from AMSU-B observations for the date of 22 March 2001. The NOGAPS analysis temperature profile was used as the background temperature. Results are shown in Figure 3, along with an infrared image for the same approximate time. Regions where the retrieval failed to converge (usually due to heavy precipitation) are left blank (e.g. the center of the intense storm near the terminus of the leftmost swath). The cloud liquid water clearly corresponds to regions of cloud in the IR image. Several extratropical cyclones and the South Pacific Convergence Zone are visible. There is an increased sensitivity to cloud near the edges of a scan, since the cloud optical depth increases with incidence angle.

The retrieval tends to put high cloud tops as expected in regions of convection in agreement with the infrared image. It also has a tendency to elevate cloud bases in these regions, perhaps due to a loss of sensitivity in heavier clouds. Realistic high cloud tops also appear on the eastern edges of extratropical

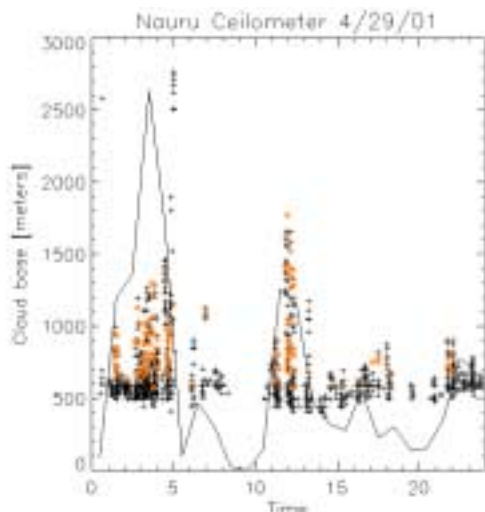


**Figure 4.** Cloud base height (black crosses) measured by a ceilometer at Nauru on 29 Apr 2001. Red crosses are the height of the second cloud base. The line indicates percentage of time within each hour that cloud was detected.

cyclones and in an area of high thin cloud west of Mexico.

### 5. VALIDATION OF RETRIEVED CLOUD PARAMETERS

Direct validation of retrieved cloud parameters has proven difficult. Several factors contribute to this difficulty. The true cloud structure may be more complicated than the simplified structure used in the simulations. Comparison with ground-based observations of cloud base height (ceilometers, METAR reports) is difficult due to disparate spatial scales (a point measurement versus an area measurement) and inexact temporal matches. (The range of cloud base heights measured by a ceilometer over just one hour can vary tremendously, as illustrated by figure 4.) Comparisons of cloud tops with infrared measurements are poor because the infrared instruments are sensing the top of the ice cloud, while the microwave is primarily sensing liquid water, and may not detect very thin clouds.

Figure 5a shows an example of retrieved cloud top height from AMSU-B observations in the North Atlantic at the same time as in Figure 3. The output of an objective geostationary infrared/visible cloud type classification algorithm (Bankert et al., 2002) is given in Figure 5b. The retrieval successfully identifies the altocumulus, altostratus, and cirrostratus (light green, dark green, and orange in Figure 5b) as high clouds. Other clouds have a tendency to be identified by the retrieval as low clouds.

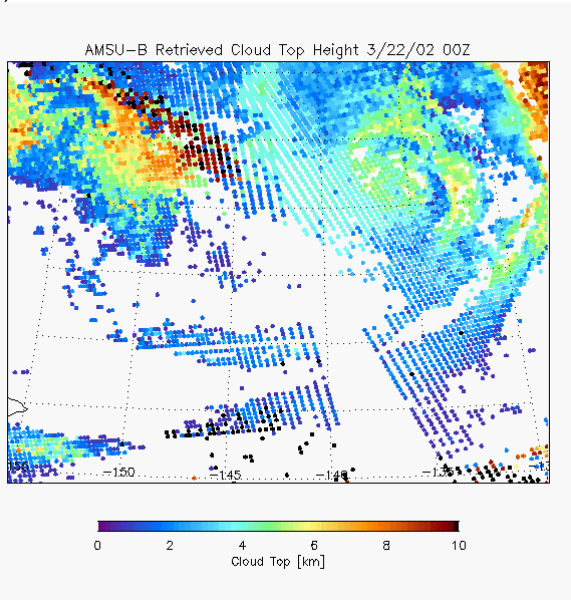
### 6. CONCLUSIONS

This algorithm seems to do well in simulation tests, but it is difficult to validate the results with real data. The future CloudSat radar (Stephens et al., 2002) could potentially be used to test and validate the quality of the retrieved cloud base information. The algorithm might also be improved by the use of additional channels. Preliminary results indicate that the retrieval of cloud liquid water is improved substantially by adding AMSU-A channels. Cloud top information from infrared sensors might help constrain the cloud position and improve cloud base retrieval.

### 7. ACKNOWLEDGEMENTS

We gratefully acknowledge the support of our research sponsors, the Office of Naval Research, Program Element (PE-060243N) and the Oceanographer of the Navy through the program office at the Space and Naval Warfare Systems Command, PMW-155 (PE-0603207N).

5a)



5b)

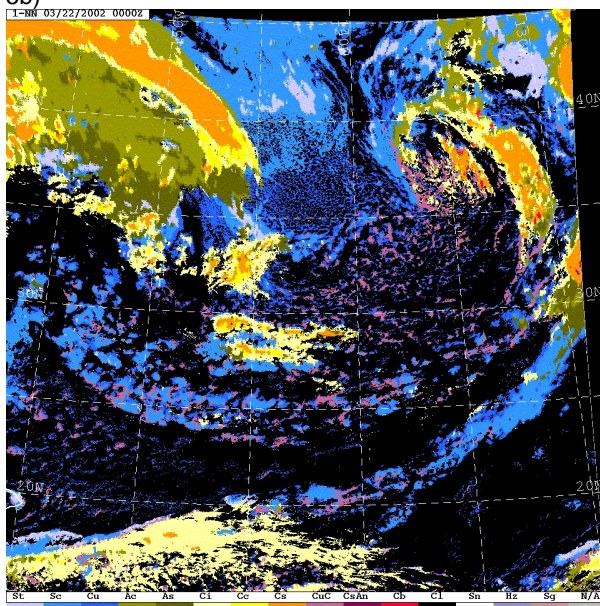


**Figure 5.** a) Retrieved cloud top height; b) Output of a cloud type classification algorithm for the same region.

## 8. REFERENCES

- Bankert, R.L., M. Hadjimichael, A.P. Kuciauskas, K.L. Richardson, J. Turk, and J.D. Hawkins, 2002: Automating the estimation of various meteorological parameters using satellite data and machine learning techniques. *Proceedings of the International Geosciences and Remote Sensing Symposium*, IEEE.
- Blankenship, C. B., A. Al-Khalaf, and T. T. Wilheit, 2000. Retrieval of water vapor profiles using SSM/T-2 and SSM/I data. *J. Atmos. Sci.*, **57**, 939-955.
- Rodgers, C.D., 2000. *Inverse Methods for Atmospheric Sounding: Theory and Practice*, World Scientific.
- Stephens, G.L., D. G. Vane, R. Boain, G. Mace, K.Sassen, Z. Wang, A. Illingworth, E. O'Connor, W. Rossow, S.L. Durden, S. Miller, R. Austin, A. Benedetti, C. Mitrescu, and the CloudSat Science Team, 2002. The CloudSat Mission and the EOS Constellation: A new dimension of space-based observations of clouds and precipitation. *Bull. Amer. Meteor. Soc.*, in press.